IEEE Access
Multidisciplinary ⋮ Rapid Review ⋮ Open Access Journal

Received 28 December 2023, accepted 13 January 2024, date of publication 22 January 2024, date of current version 1 February 2024.

Digital Object Identifier 10.1109/ACCESS.2024.3357142

RESEARCH ARTICLE

A Conflict-Aware Channel Assignment in Multi-Radio Multi-Channel Wireless Mesh Networks

DONGHOON SHIN[1], (Member, IEEE), CHANGREOL LEE[2], AND SUNGHEE CHOI[3]
[1]Department of Electrical Engineering and Computer Science, DGIST, Daegu 42988, South Korea
[2]Inzent Research and Development Center, Seoul 04516, South Korea
[3]School of Computing, Korea Advanced Institute of Science and Technology (KAIST), Daejeon 34141, South Korea

Corresponding author: Sunghee Choi (sunghee@kaist.edu)

This work was supported in part by the National Research Foundation of Korea (NRF) funded by the Korean Government (MSIT) under Grant NRF-2022R1G1A1011933, and in part by the Institute of Information & Communications Technology Planning & Evaluation (IITP) funded by the Korean Government (MSIT) under Grant 2019-0-01158.

ABSTRACT This paper proposes a theoretical model-driven channel assignment scheme designed to enhance network performance in multi-radio multi-channel wireless mesh networks. Unlike previous conflict graph-based channel assignments that addressed co-channel interference and hidden terminal problems while overlooking an exposed terminal problem, our proposed approach integrates these problems comprehensively to mitigate network performance degradation. Given a communication graph, we establish a conflict graph based on hop distance for practical implementation. The weighted conflict graph is constructed by analyzing packet collision conditions under the IEEE 802.11 standard with the CSMA/CA protocol, considering not only the transmission range and interference range but also the carrier sensing range simultaneously. Given a weighted conflict graph and available channel lists on each router, we devise a *Weighted Soft List Coloring* problem to address the channel assignment challenge. We prove the NP-hardness of this problem by establishing its dual problem, Max *list*-Cut. We present an approximation algorithm with worst-case performance at most twice the optimal solution while preserving network topology. We substantiate the performance of the proposed channel assignment algorithm through simulations in various topologies. The proposed algorithm, on average, demonstrates a network throughput increase of 162% and 174% compared to the greedy heuristic algorithm with 3 channels and 12 channels, respectively.

INDEX TERMS Channel assignment in IEEE 802.11 networks, multi-radio and multi-channel, weighted soft list coloring problem, max *list*-cut problem, approximation algorithm.

I. INTRODUCTION

Wireless mesh networks are multi-hop networks that consist of static wireless devices that connect to each other and act as routers. Since wireless mesh networks are capable of self-configuring and ad-hoc networking, they can provide wide coverage through multi-hop communication with low maintenance costs [2], [3]. Wireless mesh networks have garnered attention in various applications such as the Internet of Things (IoT), Intelligent Transport Systems (ITS), smart grids, healthcare systems, etc.

In a wireless mesh network adhering to IEEE 802.11 standards, wireless routers equipped with a single half-duplex radio typically operate on a single channel [4]. Unlike wired networks, this setup leads to signal interference among nearby communications, resulting in a significant degradation of network performance. As the number of nodes increases within a confined area, these interference issues may escalate. In order to mitigate collisions in nearby communications, the CSMA/CA (Carrier Sense Multiple Access/Collision Avoidance) protocol is employed in IEEE 802.11 networks. Despite its ability to avoid simultaneous transmissions among nearby communications, the CSMA/CA protocol introduces transmission delays

The associate editor coordinating the review of this manuscript and approving it for publication was Ronald Chang.

when operating with a single channel. Additionally, the classic problems of hidden terminals and exposed terminals persist in wireless networks using the CSMA/CA protocol. The availability of multiple non-overlapping (orthogonal) channels offers a potential solution, as it allows for increased network capacity by leveraging channels that do not interfere with each other. Furthermore, the use of different channels at hidden or exposed terminals can help prevent issues related to hidden and exposed terminals.

Ideally, it is possible to avoid the hidden terminal problem, the exposed terminal problem, and even the co-channel interference problem without any network delay by assigning all distinct orthogonal channels to each communication link. As the size and cost of radio modules have decreased in recent years, equipping wireless routers with multiple radio interfaces to enhance network performance has become more affordable. Unfortunately, the number of available non-overlapping channels is limited by IEEE 802.11 standards. For instance, only three orthogonal channels are available in the 2.4 GHz band used by IEEE 802.11b/g/n networks. In the 5 GHz band used by IEEE 802.11a/n networks, there are typically 12 or 13 orthogonal channels. The number of orthogonal channels in the IEEE 802.11ac 5 GHz band depends on the channel bandwidth and the regulatory domain. For example, with a 20 MHz channel width, there are 24 orthogonal channels available. Channel allocation problems have been extensively studied in various network environments [5], [6]. However, they have often focused on minimizing the number of necessary channels rather than minimizing interference within confined channels. In addition, the hidden and exposed terminal problems are not considered together despite their significant impact on network efficiency [4].

In this paper, we present a performance-guaranteed channel assignment scheme designed to improve network performance in multi-radio, multi-channel wireless mesh networks by collectively addressing co-channel interference, hidden terminal, and exposed terminal problems. We analyze the conditions that give rise to these issues based on the hop distance when transmission, interference, and carrier sensing ranges differ. According to these conditions, we introduce a *weighted conflict model*, which quantifies potential conflicts among communication links. We then formulate the channel assignment problem using this weighted conflict model. Our approach offers a 2-approximation algorithm for channel assignment, preserving network topology and avoiding influence on the routing protocol. Importantly, our algorithm does not rely on specific assumptions, such as particular network topologies or homogeneous networks where all routers possess the same number of radio interfaces and available channels, making it readily applicable to real-world networks.

The main contributions of this paper are as follows.

- We present weighted conflict graphs that consider co-channel interference, hidden terminal, and exposed terminal problems simultaneously for the first time. We introduce an effective conflict model based on hop distance for channel assignment in actual wireless environments, accommodating variations in carrier sensing range, interference range, and transmission range.
- We define *Weighted Soft List Coloring* to resolve the channel assignment problem for reducing conflicts while maintaining the topology when given the radio interfaces. We also define the dual problem as *Max list-Cut* to prove that the channel assignment problem is NP-hard as well as APX-hard.
- We provide an approximation algorithm for the channel assignment, guaranteeing a worst-case performance that is at most twice the optimal solution. Supported by theoretical guarantees, we validate the performance of the proposed algorithm through simulations.

This paper is the extended version of the preliminary paper [1]. The expansion encompasses a thorough proof of the NP-hardness of the given problem, incorporating hop distance rather than Euclidean distance for conflict graphs and presenting extensive simulation results along with a study of parameters. The rest of the paper is organized as follows. In Section II, we provide related work of channel assignments in multi-radio multi-channel wireless networks. In Section III, we explain how to construct conflict graphs based on wireless signal ranges. We formulate the channel assignment problems given a list of available channels in Section IV. Moreover, we offer a theoretical analysis and propose approximate algorithms. In Section V, we analyze the performance of the proposed method through simulations and conclude in Section VI.

II. RELATED WORK

In wireless networks, electromagnetic interference is a crucial factor causing network performance degradation. Co-channel interference prevents neighboring transmissions from successfully transferring data simultaneously when using a single radio interface with a single channel. The CSMA/CA mechanism, adopted in IEEE 802.11 standards, can mitigate co-channel interference by waiting for the ends of others' communications before sending. However, it yields network delay although the signals do not interfere with its transmission. Considering network throughput and delay, the channel assignment with multiple channels has been widely studied. Comprehensive surveys on channel assignment have also been conducted in the literature, such as those introduced in [7] and [8]. Islam et al. categorized evaluation metrics and approaches of previous channel assignment schemes, considering aspects such as the point of decision, dynamicity, granularity, underlying method, and the spanning layer in the OSI (Open Systems Interconnection) reference model in [8]. So and Vaidya [9] presented the dynamic channel switching scheme with multi-channel to avoid conflicts, especially the hidden terminal problem. Claude et al. [10] proposed a channel assignment scheme for fast broadcasting in

multi-channel wireless networks. However, utilizing multiple channels with a single radio interface results in substantial control overhead and necessitates time synchronization for effective communication.

As the cost of radio modules decreases, numerous studies have proposed channel assignment algorithms utilizing multi-radio and multi-channel configurations to overcome these constraints [11], [12], [13], [14]. Since the co-channel interference occurs between communication links connecting to a common router in a communication graph, coloring is often used for the channel assignment problems. Kari et al. [15] addressed the *Soft Edge Coloring* problem. They presented a distributed greedy method to assign different channels to the nearby communication links using edge coloring with a limited number of colors. Wang and Liu [16] also formulate the channel allocation problem by using coloring for open spectrum wireless networks. They considered that each node represents wireless users such as wireless lines, WLANs, or cells and edges are interference between them. Consequently, they proposed the *List-coloring* based channel assignment to prevent simultaneous sharing of the same spectrum for each node. Jain et al. [17] employed the conflict graph to model interference between wireless routers. Marina and Das [18] extended the conflict graph to the multi-radio conflict graph. They introduced topology control for reducing conflicts while keeping the network connectivity and presented the heuristic channel assignment. Katzela and Naghshineh [19] introduced several channel assignment schemes. However, these researches primarily focused only on minimizing the co-channel interference between allocated channels and often assumed homogenous networks in which each router has the same number of radio interfaces and available channels.

Despite the utilization of multiple channels and radios in the aforementioned studies, the hidden terminal problem persists. However, Hammash et al. [20] demonstrated that the hidden terminal problem is more closely related to performance degradation than the co-channel interference problem. Hao et al. [4] proposed a channel allocation method considering both co-channel interference and hidden terminal problems. They regarded a 2-hop edge as a hidden terminal condition and presented the channel assignment algorithm. However, this condition for the hidden terminal problem is only partially correct since the transmission range, carrier sensing range, and interference ranges differ in a real wireless environment, as we will explain in detail in Section III. In this paper, we investigate the conditions for the hidden terminal and co-channel interference problems when the transmission, interference, and carrier sensing ranges vary. Furthermore, we examine the condition for the exposed terminal problem and present the weighted conflict graph considering co-channel interference, the hidden terminal, and the exposed terminal problems collectively.

Unlike conventional studies that solely address the channel assignment problem, joint works with routing protocols have been proposed [21], [22], [23], [24]. This problem is also proved to be NP-hard in [23]. Since the number of channels and radio interfaces is limited to a small number in practice, Yoshihiro and Noi [22] presented the collision-free channel assignment with 3-4 available channels by incorporating a CSMA-aware interference model and partially a routing functionality. Later, Tian and Yoshihiro presented a collision-free channel assignment and routing scheme with 3-5 orthogonal channels considering traffic in [24]. Recently, channel assignment using deep reinforcement learning has been studied based on the measured throughput [25], [26], [27]. However, deep learning-based approaches still do not provide sufficient theoretical guarantees.

In contrast to prior research, we introduce weighted conflict graphs that depict potential conflicts arising from the hidden terminal, exposed terminal, and co-channel interference problems. Furthermore, we account for variations in transmission, interference, and carrier sensing ranges to mirror IEEE 802.11 network environments when constructing the conflict graph. This paper does not assume homogeneous networks, which means that each router may possess a different number of radio modules and channel lists. Utilizing the proposed weighted conflict graph, we present a channel assignment scheme that offers a theoretical foundation without relying on any specific routing protocol.

III. GRAPH MODELS FOR CONFLICTS

We present a method for modeling conflicts in wireless networks by examining the characteristics of transmission signals in IEEE 802.11 networks and deriving conflict graphs for three specific problems: the co-channel interference problem, the hidden terminal problem, and the exposed terminal problem.

A. WIRELESS NETWORK ISSUES IN THE IEEE 802.11 NETWORKS

We provide an overview of the operational context of IEEE 802.11 networks. We assume that all wireless devices (nodes) have identical transmission ranges and are equipped with multiple half-duplex radio interfaces. In IEEE 802.11 wireless networks employing CSMA/CA, we examine three signal range types to elucidate conditions related to wireless network issues.

- Transmission range(R_t): the range within which nodes can interpret signals to receive or overhear packet transmissions.
- Interference range(R_i): the range within which nodes can suffer collisions due to interference.
- Carrier sensing range(R_s): the range within which a node can detect a signal in order to recognize a transmission in progress.

Previous studies have examined the relationships among these signal ranges in commonly used IEEE 802.11 radio modules [28], [29]. Generally, these studies have identified the following relationships:

$$R_t < R_i < R_s \tag{1}$$

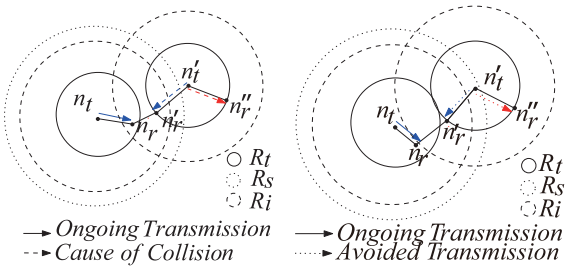

(a) The hidden terminal problem (b) The exposed terminal problem

FIGURE 1. The hidden terminal problem and the exposed terminal problem.

1) THE HIDDEN TERMINAL PROBLEM

The hidden terminal problem occurs when one receiver n_r is visible from two transmitters n_t and n'_t, but those transmitters cannot detect each other. The RTS/CTS handshaking mechanism has been addressed to resolve the hidden terminal problem. However, the hidden terminal problem barely occurs under the basic CSMA/CA protocol in the current IEEE 802.11 networks. Because the carrier sensing range is usually longer than twice the transmission range [30], [31], the transmitters can sense each other's carrier except when obstacles are between them. Thus, the transmitters naturally avoid simultaneous transmission even though the RTS/CTS technique has yet to be adopted.

Nevertheless, the hidden terminals may still exist because of the interference range [30]. As illustrated in Fig. 1(a), the transmission from n_t to n_r is broken by the transmission from n'_t to n'_r when n_r is within the interference range of n'_t. Accordingly, we define (n_t, n_r) as a hidden link of n'_t when $d(n_t, n_r) \leq R_t$, $d(n'_t, n_r) \leq R_i$, and $d(n_t, n'_t) > R_s$. This extended version of the hidden terminal problem is called a *distance terminal problem* [30].

2) THE EXPOSED TERMINAL PROBLEM

The exposed terminal problem arises when a transmitter n_t is prevented from sending data to a receiver n_r because of another transmission from n'_t to n'_r although these transmissions do not interfere each other. Regarding signal ranges, the exposed terminal problem arises when two transmitters n_t and n'_t are within the carrier sensing range, and each of the corresponding receivers n_r and n'_r are not in the interference range of the non-associated transmitters n'_t and n_t, respectively as shown in Fig. 1(b). We define (n_t, n_r) as the exposed link of n'_t when $d(n_t, n_r) \leq R_t$, $d(n'_t, n'_r) \leq R_t$, $d(n'_t, n_r) > R_i$, $d(n_t, n'_r) > R_i$, and $d(n_t, n'_t) \leq R_s$.

3) THE CO-CHANNEL INTERFERENCE PROBLEM

The co-channel interference problem frequently occurs in wireless networks, which causes a receiver not to interpret incoming signals correctly. The CSMA/CA protocol is adopted to avoid such collisions by waiting for sending until ongoing transmissions are completed. It may yield network delays unless every transmitter uses different channels. Indeed, the hidden terminal problem is also caused by co-channel interference at the receiver. In this paper, to distinguish the co-channel interference problem from the hidden terminal problem, we only consider the interference detectable by the transmitter which means two transmitters are within a carrier sensing range or each other. Consequently, the interference problem has the following conditions: $d(n_t, n_r) \leq R_t$, $d(n_t, n'_t) \leq R_s$, and $d(n_r, n'_t) \leq R_i$.

B. WEIGHTED CONFLICT GRAPHS

We propose weighted conflict graphs encompassing possible collisions caused by the aforementioned wireless problems. Since a pair of communications may induce conflicts, we design a conflict graph from the communication graph. We could more accurately predict possible conflicts if we knew the exact locations of all routers and obstacles. Since it is challenging to acquire precise locations of them in practice, there have been researches on connectivity-based localization by estimating the Euclidean distance between adjacent nodes using the signal strength [32], [33]. However, acquiring accurate Euclidean distance from the signal strength is still formidable, particularly in complex signal propagation environments or under challenging conditions. We propose a weighted conflict graph based on the hop distance in a simple environment and further extend it for practical use.

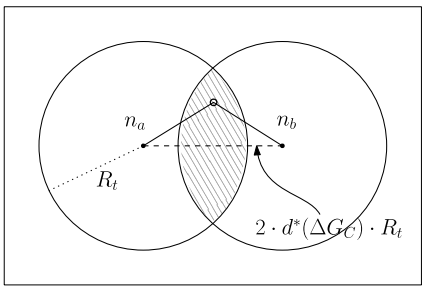

FIGURE 2. The expected maximum Euclidean distance $2 \cdot d^*(\triangle G_C) \cdot R_t$ of 2-hop distance with the network degree $\triangle G_C$.

1) A WEIGHTED CONFLICT GRAPH IN A SIMPLE ENVIRONMENT

We assume that all nodes are deployed in a 2D plane without obstacles and that all routers have identical transmission ranges. A communication graph is represented as a unit disk graph, denoted as $G_C = (V_C, E_C)$ where V_C is a set of vertices and E_C is a set of edges. A communication graph G_C is called *connected* if every pair of nodes has a routing path. We assume a deployed mesh network is connected.

Now, we explain how to build the corresponding conflict graph from a communication graph. In a communication graph G_C, an edge $(n_i, n_j) \in E_C$ indicates that nodes n_i and n_j can communicate directly. In the weighted conflict graph $G = (V, E, w)$, all edges E_C of G_C become vertices, $V = E_C$. Now, we need to define a set E of edges representing conflicts and a weight function $w(e_i)$ on every edge e_i.

We rely on hop distance as a practical alternative to address the challenge of assessing the impact of neighboring nodes on each other's transmission without complete network topology information. To understand the relationship between hop distance and Euclidean distance, especially in scenarios with randomly deployed nodes following a uniform distribution, we begin by calculating the expected Euclidean distance for a 1-hop distance. 1-hop neighbors are uniformly distributed within the disk of radius R_t.

$$E[\text{1-hop Euclidean distnace}] = \frac{\int_0^{R_t} 2\pi r\, dr}{\pi R_t^2} = \frac{2}{3}R_t \quad (2)$$

Accordingly, if n_a and n_b are c-hop neighbors of each other, we may simply estimate

$$\hat{d}(n_a, n_b) = c \cdot \frac{2}{3}R_t. \quad (3)$$

Nevertheless, one noteworthy observation is that as the node density within the network rises, the sum of the Euclidean distances along the shortest path between two nodes approaches the Euclidean distance directly between those two nodes. It suggests that network density plays a crucial role in shaping the connection between hop distance and Euclidean distance. Therefore, instead of using $\hat{d}(n_a, n_b)$, which is derived from an average distance, we employ the expected maximum Euclidean distance. Let ΔG_C be an average degree of the communication graph G_C. The average degree can be a good feature estimating the network density. Given ΔG_C, we estimate the expected maximum Euclidean distance $2d^*(\Delta G_C) \cdot R_t$ between 2-hop neighbor nodes n_a and n_b. The expected maximum Euclidean distance for 1-hop $d^*(\Delta G_C)$ can be computed by

$$\frac{\pi}{\Delta G_C} = 2(\arccos d^*(\Delta G_C) - d^*(\Delta G_C)\sqrt{1-d^*(\Delta G_C)^2}) \quad (4)$$

as shown in Fig. 2. Assuming a uniform distribution, we can infer the probability of nodes being present in the intersection area of the transmission ranges of two nodes as the network degree. When $R_t = 1$ (not necessarily set to 1), the left side of the equation 4 represents the area of the circle divided by the degree, and the right side calculates the intersection area. Let R_c be the expected maximum Euclidean distance between two nodes whose hop distance is c. We can approximate R_c by $\max(c \cdot d^*(\Delta G_C)R_t, c \cdot \frac{2}{3}R_t)$. In the sparse network, we take the average distance since $d^*(\Delta G_C)$ becomes relatively smaller. Fig. 3 shows the expected maximum Euclidean distance $d^*(\Delta G_C)R_t$ for 1-hop by an average degree ΔG_C of the network.

According to the conditions for occurring the network problems described in the previous section, we need to calculate how far the interference range and sensing range can affect in terms of hop distance. We compute the maximum hop distances influenced by interference and carrier sensing ranges as follows:

$$C_i = \arg\max_c \{R_c | R_c \le R_i\} \quad (5)$$

$$C_s = \arg\max_c \{R_c | R_c \le R_s\} \quad (6)$$

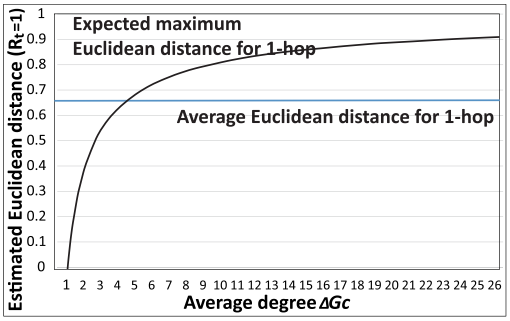

FIGURE 3. The expected maximum Euclidean distance for 1-hop by an average degree of the network.

Now, we explain how to add conflict edges to the conflict graph. First, we calculate the hop distance between all pairs of vertices from the communication graph. Let $d_h(n_i, n_j)$ be a hop distance between n_i and n_j. We select a pair of two vertices $v_i = (n_t^i, n_r^i)$ and $v_j = (n_t^j, n_r^j)$ from the conflict graph G. If $d_h(n_t^j, n_r^i) \le C_i$ or $d_h(n_t^i, n_r^j) \le C_i$, we add an edge between v_i and v_j. Additionally, we check whether $d_h(n_t^i, n_t^j) > C_s$. If true, we label the edge as a hidden edge H; otherwise, we label it as an interference edge I. If $d_h(n_t^j, n_r^i) > C_i$, $d_h(n_t^i, n_r^j) > C_i$, and $d_h(n_t^i, n_t^j) \le C_s$, we add an edge between v_i and v_j and label it as an exposed edge E. The same procedure is applied for communication in the opposite direction. When generating conflict edges, if there is an existing edge, we simply add a label without creating a new edge. Performing this process for every pair of vertices results in the creation of the conflict graph.

At this point, we have a conflict graph consisting of conflict edges labeled as H, I, and/or E and all transmission links in G_C as vertices in G. We describe the process of assigning weights to each edge. The edges signify conflicts between two concurrent transmissions, meaning such conflicts arise when n_t' attempts to send a signal while n_t is transmitting. The frequency of conflicts is represented by $P(n_t) \cdot P(n_t')$, where $P(n_t)$ and $P(n_t')$ denote the probabilities of transmission for n_t and n_t', respectively. We assign $\alpha \cdot P(n_t) \cdot P(n_t')$ to the interference conflict edges, $\beta \cdot P(n_t) \cdot P(n_t')$ to the hidden conflict edges, and $\gamma \cdot P(n_t) \cdot P(n_t')$ to the exposed conflict edges. Here, α, β, and γ serve as weights determined by the importance assigned to each problem.

To generate the conflict graph, we calculated the shortest hop distance for every pair of vertices in the communication graph. This can be computed using the Floyd-Warshall Algorithm in $O(|V_C|^3)$ time. Since the number of vertices in the conflict graph is at most $|E_C|$, calculating conflict edges between all pairs of vertices in the conflict graph requires a maximum of $O(|E_C|^2)$ time and space.

2) A WEIGHTED CONFLICT GRAPH IN PRACTICE

For practical use, we propose a method to simplify conflict graph generation through strong assumptions about signal ranges. We assume that transmission, interference, and carrier

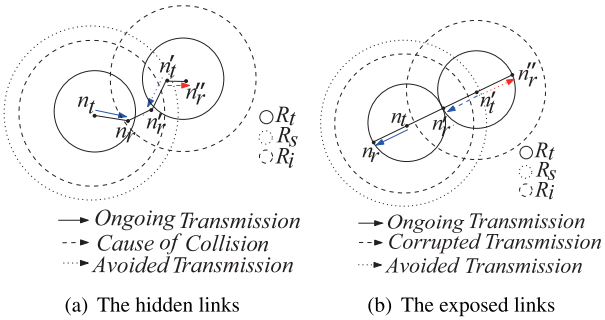

(a) The hidden links (b) The exposed links

FIGURE 4. (a) 3-hop links but not 2-hop links are hidden. (b) 3-hop links but not 2-hop links are exposed.

sensing ranges have the following relations [30].

$$R_t < R_i = 1.778R_t < R_s = 2.2R_t \tag{7}$$

Since we investigate conflicts among communication links, we define *k-hop links* as two edges whose minimum hop path passes k routers excluding two end nodes. If two edges are adjacent, having one shared vertex, it is a 1-hop link.

Now, we consider the conflicts between a pair of communication links. In the case of the hidden terminal problem, two transmitters are apart more than twice the transmission range because $R_s = 2.2\ R_t$. Thus, the hidden terminal problem cannot arise at 1-hop links. As shown in Fig. 1(a), there is a conflict between (n_t, n_r) and (n'_t, n'_r) since n_r lies within an interference range of n'_t. Two links (n_t, n_r) and (n'_t, n'_r) are 2-hop links. (n_t, n_r) is a hidden link of (n'_t, n'_r). Moreover, (n_t, n_r) is still a hidden link of (n'_t, n''_r) which means 3-hop links including (n'_t, n'_r) can be associated with the hidden terminal problem. Thus, a conflict may occur at 3-hop links. However, the opposite argument does not always hold. Although 3-hop links have a collision by the hidden terminal problem, 2-hop links, which is a subpath of the 3-hop links, may not suffer from the hidden terminal problem. It is because two end nodes of the 2-hop links can be within $2.2R_t$ as shown in Fig. 4(a). In the case of the exposed terminal problem, two transmitters n_t and n'_t are within a carrier sensing range of each other, and each receiver n_r and n'_r are not within an interference range of the non-associated transmitter as shown in Fig. 1(b). It implies that two exposed links should be at least 2-hop links. A conflict occurs if n_t and n'_t send a packet simultaneously. If two links (n_t, n_r) and (n'_t, n'_r) are 2-hop links and (n_t, n_r) is the exposed link of (n'_t, n'_r), (n_t, n_r) is still the exposed link of (n'_t, n''_r) as shown in Fig. 1(b). It means that 3-hop links containing 2-hop links suffering the exposed terminal problem also suffer from the exposed terminal problem, although the opposite does not hold, as shown in Fig. 4(b). In the previous section, we found the conditions for the interference problem, which are $d(n_t, n_r) \leq R_t$, $d(n_t, n'_t) \leq R_s$ and $d(n_r, n'_t) \leq R_i$. Accordingly, 1-hop, 2-hop, and even 3-hop links can be involved in the interference problem unless they are related to the hidden or exposed terminal problem.

Based on the observations above, the following three arguments hold:

- 1-hop links are only affected by interference, not by the hidden or exposed terminal problem.
- If 2-hop links are affected by the hidden or exposed terminal problem, induced 3-hop links are also affected by the hidden or exposed terminal problem.
- Up to 3-hop links, they suffer from at least one problem among the interference problem, hidden terminal problem, and exposed terminal problem.

The first two claims are obvious from the above explanation. We prove the third claim simply with the exposed terminal problem and the interference problem. At 1-hop links, it is obvious that the interference problem occurs when two nodes send a packet to a common receiver. At 2-hop links of which path consists of 4 routers, $n_1, \ldots, n_4$, it is obvious that n_2 is within a carrier sensing range of n_3. When n_2 sends a packet to n_1 and simultaneously n_3 sends a packet to n_4, those two transmissions suffer from either the exposed terminal problem or the interference problem. If n_1 is not within an interference range of n_3 and n_4 is not within an interference range of n_2, two transmissions have the exposed terminal problem. Otherwise, they suffer from the interference problem. At 3-hop links of which path consists of 5 routers, $n_1, \ldots, n_5$, two transmissions n_2 to n_1 and n_4 to n_5 have the same problem because n_2 is still within a carrier sensing range of n_4 as shown in Fig. 4(b). Consequently, we can guarantee that 1-hop, 2-hop, and 3-hop links are influenced by at least one of the hidden terminal, exposed terminal, and co-channel interference problems.

We construct a weighted conflict graph $G = (V, E, w)$ from a communication graph $G_C = (V_C, E_C)$. Each edge in G_C becomes vertices of G, $V = E_C$. The edges of the conflict graph are defined as

$$E = \{(l_i, l_j) \mid l_i \text{ and } l_j \text{ are within 3-hop where } l_i, l_j \in V\}.$$

The weight of each edge represents how critical each conflict is. It seems that 1-hop links are related to the interference problem, 2-hop links are related to the hidden terminal problem, and 3-hop links are mainly related to the exposed terminal problem if the nodes are well distributed. Thus, the weight of each edge is assigned according to link distance.

$$w((l_i, l_j)) = \begin{cases} \alpha & \text{if } l_i, l_j \text{ are adjacent,} \\ \beta & \text{if } l_i, l_j \text{ are 2-hop links,} \\ \gamma & \text{if } l_i, l_j \text{ are 3-hop links.} \end{cases}$$

Fig. 5(a) and Fig. 5(b) show the weighted conflict graph corresponding to the communication model.

As in the previous section, the cost and time required to generate the conflict graph remain $O(|V_E|^2)$. This is because the number of conflict edges can be generated up to a maximum of $O(|V_E|^2)$.

IV. CONFLICT-AWARE CHANNEL ASSIGNMENT

In this section, we introduce a channel assignment algorithm aimed at conflict reduction. We define a *Weighted Soft*

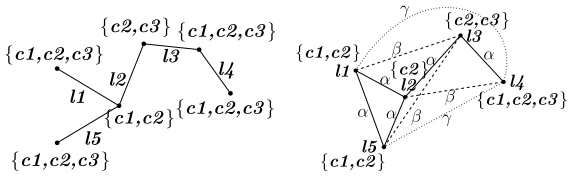

(a) A communication graph (b) A weighted conflict graph

FIGURE 5. A communication graph with channel lists and the corresponding weighted conflict graph.

List Coloring problem, which is closely tied to channel assignment, and its dual problem, Max *list*-Cut. Additionally, we present a 2-approximation algorithm for Max *list*-Cut, specifically designed for addressing the channel assignment problem.

A. PROBLEM STATEMENT

We define a *Weighted Soft List Coloring* problem of which solution can be directly applied to a channel assignment problem. It is often impossible to allocate entirely unique channels to every link, primarily due to limitations in the number of radio modules each router can accommodate and the restricted availability of channels. Therefore, we begin by evaluating the available channel set for each link. On the communication graph, this set is composed of the common channels used by the two end routers connected by the link. Therefore, on the weighted conflict graph, each vertex shares the same set of available channels as the corresponding link on the communication graph, as shown in Fig. 5(a) and Fig. 5(b). Let $L(v)$ be the list of available channels at v.

$$L(v) = L(n_i) \cap L(n_j) \text{ where } v = (n_i, n_j) \in V \text{ and } n_i, n_j \in V_C \tag{8}$$

Consequently, a vertex coloring problem on the weighted conflict graph can solve a channel assignment problem.

1) WEIGHTED SOFT LIST COLORING

Our objective is to assign a color to each vertex such that the total weight of monochromatic edges is minimized where the monochromatic edge is defined as the edge whose both end vertices are colored the same.

Given an undirected weighted graph $G = (V, E, w)$ with a color(channel) list of each vertex $L(v)$ for $v \in V$, and with a weight of each edge $w(e)$ for $e \in E$, a *Weighted Soft Coloring Problem* is defined as

$$\text{Compute } c(v) \in L(v) \text{ to minimize } \sum_{e \in M} w(e) \tag{9}$$

where $M = \{(u, v) \mid c(u) = c(v), (u, v) \in E\}$ and $c(v)$ is a chosen color at v among $L(v)$.

2) MAX *LIST*-CUT

We define the Max *list*-Cut problem, which is a dual problem of the *Weighted Soft List Coloring* problem, to prove NP-hardness and present an approximation algorithm for the channel assignment. Since the total weight of a conflict graph is equal to the sum of the weights of monochromatic and non-monochromatic(dichromatic) edges, we derive a dual maximizing problem, Max *list*-Cut Problem. Given an undirected weighted graph $G = (V, E, w)$ with a partition list of each vertex $L(v)$ for $v \in V$ and a weight of each edge $w(e)$ for $e \in E$, the Max *list*-Cut problem is defined as

$$\text{Compute } c(v) \in L(v) \text{ to maximize } \sum_{e \in X} w(e) \tag{10}$$

where $X = \{(u, v) \mid c(u) \neq c(v), (u, v) \in E\}$.

The objective of the Max *list*-Cut problem is to maximize the total weight of edges whose two end vertices belong to different partitions.

Theorem 1. *The Max list-Cut problem is NP-hard.*

Proof: We prove this by the reduction of the *Max k-Cut* problem, which is a well-known NP-hard problem. Given a constant k and a weighted graph $G = (V, E, w)$ where V, E, and $w(e_i)$ are a set of vertices, a set of edges, and a weight function on an edge $e_i \in E$, *Max k-Cut* asks to divide the vertices into k partitions such that the sum of weights of edges crossing different partitions is maximized. The Max k-Cut problem can be polynomial-time reducible to the Max *list*-Cut problem by configuring that all vertices have the identical partition list of size k in the Max *list*-Cut problem. Since the objective of Max *list*-Cut is to maximize the sum of weights of edges crossing partitions, the answer to the problem can be directly applied to the solution for the Max k-cut problem. The Max *list*-Cut problem is indeed a generalized version of a *Max k-Cut* problem. Since the Max k-Cut problem is known to be NP-hard, the Max *list*-Cut problem is NP-hard. ■

The Max k-Cut problem is also known to be APX-hard; we cannot have an algorithm with an approximation ratio better than $1 - \frac{1}{34k}$ unless P=NP [34]. From Theorem 1, we can infer that given the channel list on each vertex, the channel assignment problem is very challenging to result in approximation schemes close to the optimal solution.

B. AN APPROXIMATION ALGORITHM FOR MAX LIST-CUT

In this section, we propose a simple greedy approximation algorithm for the Max *list*-Cut problem with performance guarantees of at least 2.

Given a weighted graph with a partition list on each vertex, the proposed algorithm GA partitions every vertex to maximize the total weight of crossing edges as described in Fig. 6. GA consists of two steps. In the first step (lines 3-6 in Fig.6), GA identifies vertices that have an available partition (channel) list of size 1. In such cases, the vertices are assigned to their respective available partition to maintain connectivity. In the second step (lines 7-10 in Fig.6), we sequentially select a vertex u and greedily assign it to a partition, choosing the partition that minimally increases the weights of edges connecting to vertices inside the partition. The algorithm ensures that each vertex is assigned to exactly one partition, as it processes each vertex one by one and places it into

Algorithm 1 GA($G = (V, E, w)$)

Input: $G = (V, E)$ with $L(v)$ for $v \in V$ and $w(e)$ for $e \in E$
Output: c(v) maximizing total weight of crossing edges

1: **for all** partition P_x **do**
2: $P_x = \emptyset$ // empty set
3: **for all** $v \in V$ **do**
4: **if** $|L(v)| = 1$ **then**
5: Add v to P_i where $L(v) = \{i\}$
6: Delete v from V
7: **for all** $u \in V$ **do**
8: **for all** partition P_i in $L(u)$ **do**
9: $W_{P_i}(u) = \sum w(e)$ where $e = (u, v), v \in P_i$
10: Add u to P_i where $i = \arg\min_{i \in L(u)} W_{P_i}(u)$
11: Assign $c(v) = i$ where $v \in P_i$ for all v

FIGURE 6. Algorithm: Greedy approximation.

a specific partition once. Fig. 7 shows how the proposed algorithm assigns colors to each vertex.

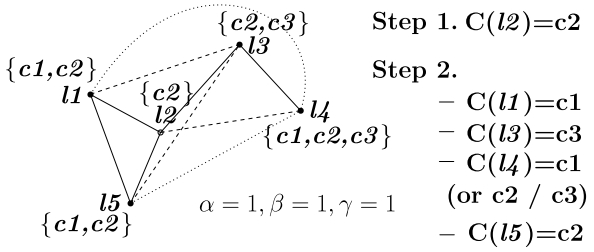

FIGURE 7. In the first step, the algorithm selects vertices who have only 1 available channel and assigns it. In the second step, the algorithm chooses vertices one by one and assigns the channel to minimize the conflicts. When $l4$ is selected, the algorithm can assign any of the channels $c1, c2, c3$ since their impacts are the same when $\alpha = \beta = \gamma = 1$. Once $c(l4) = c1$, $c(l5) = c2$ because $l5$ has 2 neighbors with a channel $c1$.

Theorem 2. *GA assigns all vertices to partitions with an approximation ratio of 2.*

Proof: We consider a set S_1 of vertices which are assigned at the first step. Let $G_{S1} = (V_{S1}, E_{S1})$ be a subgraph where $V_{S1} = S_1$ and $E_{S1} = \{(u, v) \in E | u, v \in V_{S1}\}$. Let W_{in}^{S1} be the total weight of edges whose ends are in the same partition in G_{S1}. Let W_{out}^{S1} be the total weight of edges across different partitions in G_{S1}.

Now, we consider the second step. Let u_i be the ith vertex partitioned at the second step. Let $G_{S2}^i = G_{S2}^{i-1} \bigcup (u_i, E_i)$ where $E_i = \{(u_i, v) \in E | v \in G_{S2}^{i-1}\}$ and $G_{S2}^0 = G_{S1}$. We consider the edges included in G_{S2} after u_i is partitioned. Let w_{in}^i be the total weight of edges in E_i whose ends are in the same partition. Let w_{out}^i be the total weight of edges in E_i whose ends are not in the same partition. Since GA assigns u_i to the partition in which the total weight of edges newly included is minimized, we have

$$w_{in}^i \leq \frac{1}{|L(u_i) - 1|} w_{out}^i. \quad (11)$$

Let $m = \max(\min_{u_i \in V \setminus V_{S1}}(|L(u_i)|), 2)$. Indeed, any vertex at the second step has a partition list of size at least 2. If we sum up values for all the vertices in the second step, we have

$$W_{in}^{S2} = \sum_{u_i \in V \setminus V_{S1}} w_{in}^i \leq \frac{1}{m-1} \sum_{u_i \in V \setminus V_{S1}} w_{out}^i = W_{out}^{S2}. \quad (12)$$

Now, we have the following inequality.

$$W_{in}^{S2} + W_{out}^{S2} + W_{out}^{S1} \leq \frac{m}{m-1} W_{out}^{S2} + \frac{m}{m-1} W_{out}^{S1}. \quad (13)$$

The total weight of edges W is equal to $W_{in}^{S1} + W_{out}^{S1} + W_{in}^{S2} + W_{out}^{S2}$, so $W_{in}^{S2} + W_{out}^{S2} + W_{out}^{S1} = W - W_{in}^{S1}$. Since the total weight OPT of edges across partitions by the optimal algorithm is always less than or equal to $W - W_{in}^{S1}$, we have

$$OPT \leq W - W_{in}^{S1} \leq \frac{m}{m-1}(W_{out}^{S1} + W_{out}^{S2}). \quad (14)$$

Since the total weight ALG of edges across partitions by the proposed algorithm is $W_{out}^{S1} + W_{out}^{S2}$,

$$OPT \leq \frac{m}{m-1} ALG. \quad (15)$$

Since $m \geq 2$, even if $\min_{v \in V} |L(v)| = 1$, we have the performance guarantee $\frac{1}{2}$. ■

The algorithm GA runs in $O(|V|^2) = O(|E_C|^2)$ time since the number of the elements of all the partitions is at most $|V|$ in the second step (lines 8-9). It requires $O(|E_C| + k)$ space where k is the maximum number of partitions.

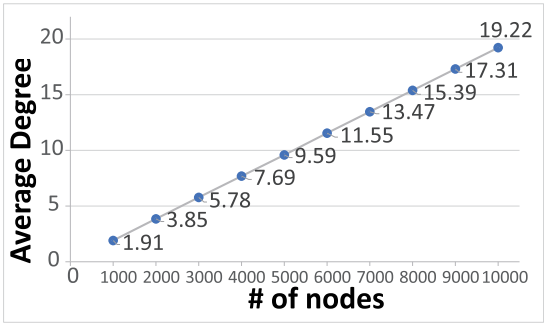

FIGURE 8. Variation in the average degree of the network with changing node numbers from 1000 to 10000.

Since all vertices belong to one of the partitions in their partition list as a result of the proposed algorithm, we can assign corresponding channels to every communication link in the communication graph. Consequently, the algorithm preserves the network topology.

V. PERFORMANCE ANALYSIS

Since we employ the hop-based distance instead of Euclidean distance when constructing a conflict graph, we first examined the relation between those distances regarding network density. In the proposed scheme, we exploit the average degree of the network to estimate the network density. Under the assumption that nodes are randomly deployed, it is a

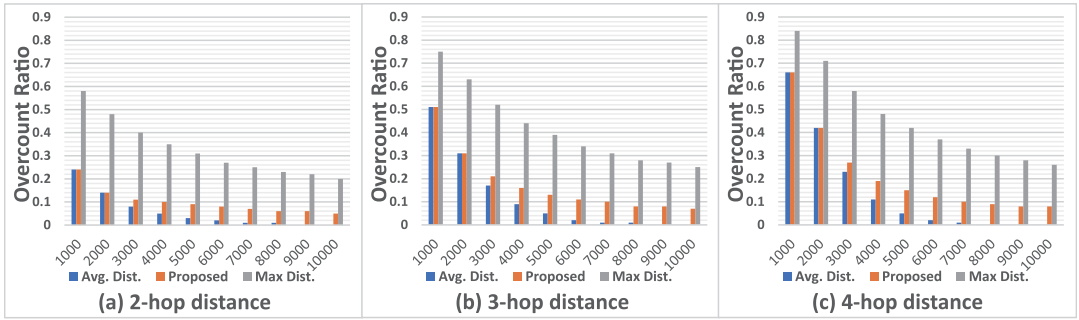

FIGURE 9. Overcount ratios for 2-hop, 3-hop, and 4-hop distances when employing average Euclidean distance, the proposed distance, and maximum Euclidean distance.

simple and effective way to estimate the density, as shown in Fig. 8. In our simulation, we placed nodes randomly within a square area with a side length of 4000 m. We varied the number of nodes from 1000 to 10000, increasing by 1000 nodes, and set the communication range of each node to 100 m. We conducted each simulation 10 times and computed an average degree. Fig. 8 shows that the average degree of the network is likely to be linear to the number of nodes, indicating the density of the network.

In Subsection III-B1, we proposed the expected maximum Euclidean distance R_c for c-hop distance. We compared the proposed distance with the average Euclidean distance $c \cdot \frac{2}{3}R_t$ and the maximum Euclidean distance $c \cdot R_t$. We examined the undercount ratio, which is calculated by the number of nodes in c-hop distance within each estimated distance over the total number of nodes in c-hop distance. Fig. 10 presents simulation results for 1-hop, 2-hop, 3-hop, and 4-hop distances. When using the maximum distance, the undercount ratio is 1 because every node is included in all cases. When using the average distance, the corresponding ratio slightly increased with the growth of hop count. However, as the network density increased, it was observed that the undercount number also increased. In the case of using the proposed distance, although undercount occurs, it is noteworthy that as the density increases, the miscount number decreases. Additionally, observing that the miscount number decreases further as the hop distance increases, it appears that using this distance instead of the maximum distance may yield positive effects. Fig. 9 illustrates the overcount ratio, calculated as the number of nodes outside the c-hop distance concerning the estimated distance over the total number of nodes counted. For a 1-hop distance, the overcount ratio is 0 since all estimated distances are less than or equal to the communication range R_t. Subsequently, Fig. 9 depicts the overcount ratio for 2-hop, 3-hop, and 4-hop distances. When employing the average distance, the achieved overcount ratio is the lowest. Although the proposed method exhibits lower performance than the method using the average distance, it tends to significantly decrease as the density increases. When using the maximum distance, there are advantages in the undercount aspect; however, from the overcount perspective, a significantly high overcount ratio occurs as the hop count increases. The simulation results suggest that the proposed method is an appropriate approach when considering both overcount and undercount aspects simultaneously.

We conducted experiments on preserving topology when allocating channels based on a simple greedy algorithm. While varying the available radio interfaces for each node from 2 to 6, we greedily assigned channels to minimize collisions with neighboring nodes on the communication graph. We assumed the number of non-overlapping channels is not limited. Fig. 11 illustrates the topology-preserving ratio, which is computed by the number of alive edges in the communication graph over the total number of edges in the communication graph. As the number of radio interfaces increased, demonstrating better performance in terms of coverage due to a higher number of available channels while the performance degradation occurred with an increase in network density. Particularly, when using only two channels, in a scenario with 10,000 nodes deployed, around 16 percent of communication edges were unable to be utilized. On the contrary, the proposed channel assignment focuses on preserving the topology. Although collisions may increase, maintaining the topology can ensure the preservation of crucial links and potentially reduce network delays. To assess network latency caused by communication link deletions, we investigated the hop distance ratio for all pairs of vertices compared to the original communication graph, as shown in Fig. 12. In our experiments, we observed an increase in hop distance between a pair of nodes when using fewer radio interfaces due to a significant number of unavailable communication links. However, we noticed that the network delay tends to be mitigated as the network density increases when using 2 radio interfaces, as more alternative paths become available. Nonetheless, maintaining the topology poses a crucial challenge, as important communication links may still be removed.

We assessed the performance of the proposed channel assignment algorithm, GA, using the NS3 simulator [35]. Wireless nodes were deployed in various topologies, and we randomly selected 5 pairs of sources and sinks. Each

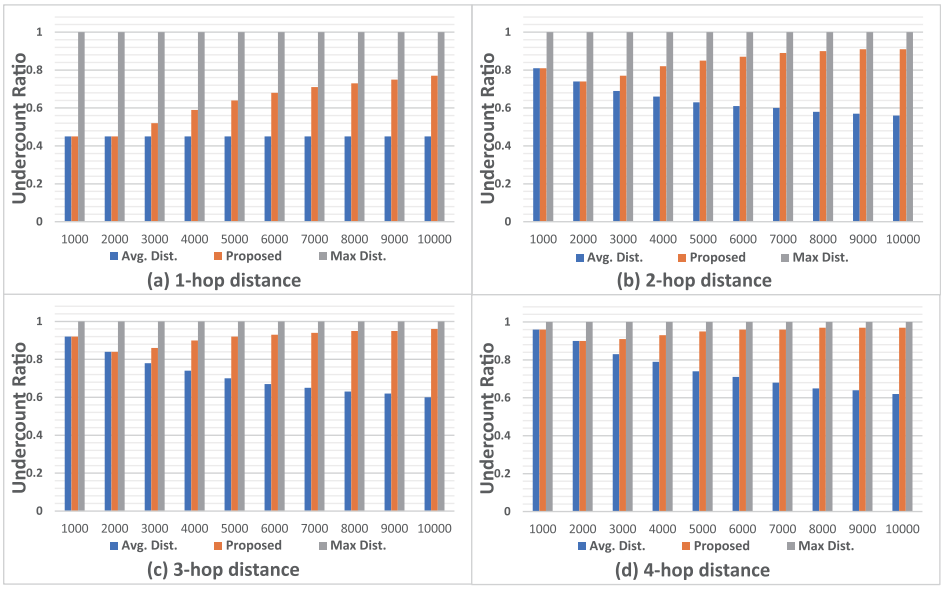

FIGURE 10. Undercount ratios for 1-hop, 2-hop, 3-hop, and 4-hop distances when employing average Euclidean distance, the proposed distance, and maximum Euclidean distance.

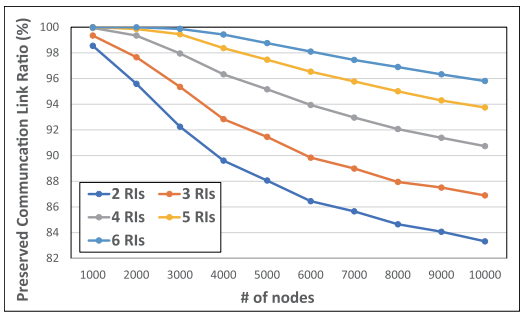

FIGURE 11. The preserved communication link ratio when channels are assigned greedily with 2 to 6 radio interfaces.

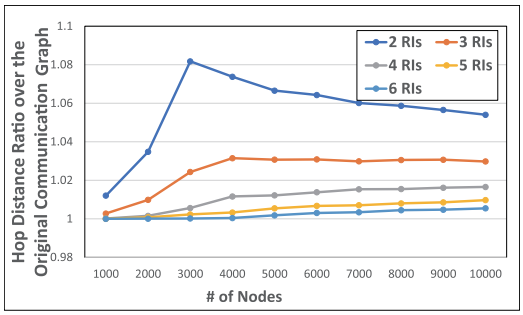

FIGURE 12. Average hop distance ratio in the resulting graph compared to the original communication graph for all pairs of vertices. If the ratio is equal to 1, there is no delay caused by the deletion of links.

source transmitted UDP packets with a size of 1024 bytes, and we recorded the successfully transmitted packets between a source and its corresponding destination. OLSR served as the routing protocol, and we allocated 30 seconds for initialization to establish a routing table. Each simulation ran for 100 seconds. Transmit power was adjusted as the transmission range, interference range, and carrier sensing range were set to 100 m, 180 m, and 220 m, respectively. We assumed signal attenuation based on the log-distance propagation model and considered homogeneous networks with up to 12 orthogonal channels. The remaining simulation settings followed the 802.11 standards provided by NS3. The table 1 summarizes several parameters.

TABLE 1. Simulation parameters.

Parameter	Value	Description
R_t	100 m	transmission range(meter)
R_i	180 m	interference range(meter)
R_s	220 m	carrier sensing range(meter)
Packet size	1024 bytes	UDP packet
Data rate	256 kbps	Except data rate variation simulations, 256 (kilobits per second) is used
Routing protocol	OSLR	Optimized Link State Routing Protocol runs 30 seconds at the initialization
# of channels	3 or 12	Except channel variation simulations, 3 or 12 channels are mostly used
(α, β, γ)	(1, 2, 2)	Weights in conflict graphs

The proposed algorithm, GA, operates on a weighted conflict model. In this simulation, we takes the weighted conflict graph proposed in Section III-B2. After constructing the conflict graph, determining the weights of α, β, and γ becomes necessary. In order to find suitable values for these parameters, simulations were conducted with various parameters in three different topologies: square lattice, triangular lattice, and random. In a square lattice and a triangular lattice, we placed 100 nodes in a 10 by 10 arrangement with three different side lengths: 50 m, 70 m, and 90 m. For a random topology, 20, 30, 40, and 50 nodes were randomly positioned in a square region with a side length of 300m In order to examine the impact of α, β, and γ, experiments were conducted by setting the same weight

TABLE 2. Simulation results with various parameters (α, β, γ) in three different topologies: square lattice, triangular lattice, and random.

α, β, γ			1,1,1	1,1,2	1,2,1	2,1,1	1,2,2	2,1,2	2,2,1	1,2,3	1,3,2	2,1,3	2,3,1	3,1,2	3,2,1
Topoloty		CHs													
Square Lattice	90m	3	**128.06**	**134.29**	112.26	54.02	121.17	**124.48**	106.34	**149.5**	**162.14**	102.85	104.78	121.65	61.7
		12	248.27	219.22	209.47	237.57	248.02	253.49	**254.59**	**253.95**	252.58	249.63	**254.96**	**254.77**	**254.61**
	70m	3	53.42	**131.76**	**113.55**	51.86	**125.33**	**117.34**	52.9	**119.98**	102.24	79.6	50.69	53.76	55.63
		12	183.55	**205.89**	**210.61**	151.17	**227.41**	**189.87**	150.85	171.1	**230.74**	179.97	155.38	148.18	130.13
	50m	3	**103.23**	**109.62**	63.39	57.65	**96.24**	50.82	47.65	62.45	**104.58**	**87.5**	49.46	48.03	64.48
		12	153.84	**228.67**	136.37	114.9	**213.97**	**193.71**	128.29	**224.93**	**210.14**	178	123.26	105.06	105.36
Triangular Lattice	90m	3	113.31	**158.43**	**143.46**	59.82	**166.26**	97.33	103.52	**140.46**	**156.16**	65.44	60.06	91.82	76.14
		12	253.44	**255.18**	245.68	**254.38**	233.07	**255.01**	239.89	249.87	**254.37**	243.74	241.34	**253.82**	216.02
	70m	3	**125.89**	**120.27**	**144.1**	35.82	**96.1**	85.55	69.66	**100.11**	79.46	86.91	90.75	36.24	48.58
		12	169.65	**245.73**	**241.22**	143.2	**251.16**	208.64	143.22	**244.02**	**242.13**	192.88	113.95	182.51	180.99
	50m	3	**59.36**	**61.89**	58.27	**60.45**	**115.96**	44.59	44.61	**113.76**	52.4	49.44	43.97	53.14	41.97
		12	134.24	157.34	**181.86**	53.98	**248.84**	135.76	58.99	**200.38**	**214.02**	**173.84**	65.76	122.11	79.17
Random	20	3	83.26	91.78	**106.32**	81.87	**117.97**	87.73	97.28	**149.86**	**122.26**	87.12	**106.53**	78.64	103.81
		12	190.75	**255.06**	210.86	211.3	**254.45**	161.49	212.46	**254.18**	**254.9**	**246.74**	211.22	165.46	211.49
	30	3	187.78	**222.66**	144.11	142.78	**228.99**	143.98	143.6	**254.35**	**190.1**	**216.27**	178.32	142.83	143.25
		12	226.78	**254.8**	254.43	228.51	**255.2**	**254.62**	214.86	**254.93**	**255.23**	254.38	217.9	178.34	184.14
	40	3	**105.1**	**66.91**	56.14	34.1	**102.22**	42.03	38.46	51.15	**98.22**	**123.25**	36.72	42.75	50.94
		12	167.57	**241.06**	**213.6**	88.03	**248.37**	163.01	100.16	**177.01**	**255.09**	133.54	89.39	165.62	111.26
	50	3	156.5	156.19	145.23	111.65	**157.3**	**160.1**	114.02	**168.37**	**159.15**	**168.42**	126.56	117.5	112.85
		12	162.66	221.55	**250.38**	139.18	**254.14**	149.74	104.34	**227.26**	**254.74**	**239.06**	173.73	172.83	101.38
Count			5	15	9	2	17	7	1	16	16	7	2	2	1

for each. After that, we simulated several testing scenarios where each factor was applied either high or low. Finally, experiments were performed with different weights for each factor. In this experiment, we employed 3 or 12 channels, which are commonly used in IEEE 802.11 protocols with 2.4 GHz or 5 GHz. Table 2 presents the average throughput when randomly configuring 5 pairs of sources and sinks, with packets transmitted at 256 kbps. In the table, the top 5 high throughputs for each scenario are highlighted in bold. The count in the last column indicates how many times each parameter combination entered the top 5 in various experiments. The experimental results show that the parameter combination (α, β, γ)=(1,2,2) occurred 17 times out of 20, (1,2,3) and (1,3,2) each occurred 16 times, and (1,1,2) occurred 15 times. In contrast, (2,2,1), (2,3,1), (3,1,2), and (3,2,1) were measured 2 times or fewer. Based on these results, we concluded that α has a relatively low impact compared to β and γ. This inference is drawn from the fact that in the weighted graph, α is only applied to 1-hop links, and in the case of 1-hop links, it is assumed to be related only to co-channel interference. In the rest of our simulation, we use the simple weighted conflict graph and set α, β, and γ to 1, 2, and 2, respectively.

Due to the absence of algorithms addressing hidden terminal, exposed terminal, and interference problems simultaneously, we developed a greedy heuristic algorithm, GH, for comparisons. Following a strategy similar to common channel assignment methods [11], GH greedily assigns unused channels to the edges of the communication graph one by one, preventing conflicts with incident edges as long as there are available channels. In cases where no unused channels are left, GH randomly assigns channels to edges.

We present the network performance with an increasing number of available channels and investigate the impact of the RTS/CTS mechanism when communication, interference, and carrier sensing ranges differ. We assume the presence of 100 nodes arranged in a 10 by 10 square lattice with a side length of 90 m. Fig. 13(a) illustrates the average throughput of sink nodes as the number of available channels varies, up to 12. In all cases, there is a tendency for higher throughputs with an increasing number of available channels. Given that our GH algorithm assigns channels to each link to minimize collisions among neighboring links on the communication graph, it exhibits high performance with a larger number of channels. However, GA outperforms GH as it can handle hidden/exposed terminal problems that arise through multi-hop neighbors. The performance with RTS/CTS appears to be lower than without RTS/CTS due to the additional control overhead it requires. Furthermore, RTS/CTS is ineffective in preventing the hidden terminal problem when the interference range surpasses the transmission range, as explained in Section III. Therefore, we disable the RTS/CTS mechanism in the following simulations.

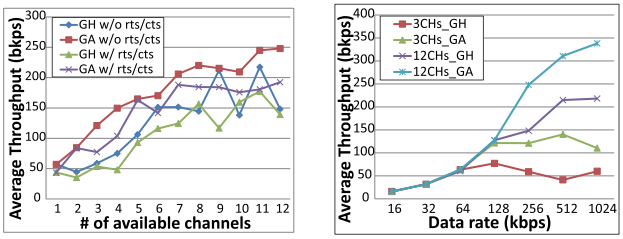

(a) (b)

FIGURE 13. Network performance in a square lattice: (a) average throughput with the various number of available channels (b) average throughput with different data rate.

Fig. 13(b) illustrates the network performance with various data rates in the previously mentioned topology. We increase the data rate of each source node from 16 kbps to 1024 kbps.

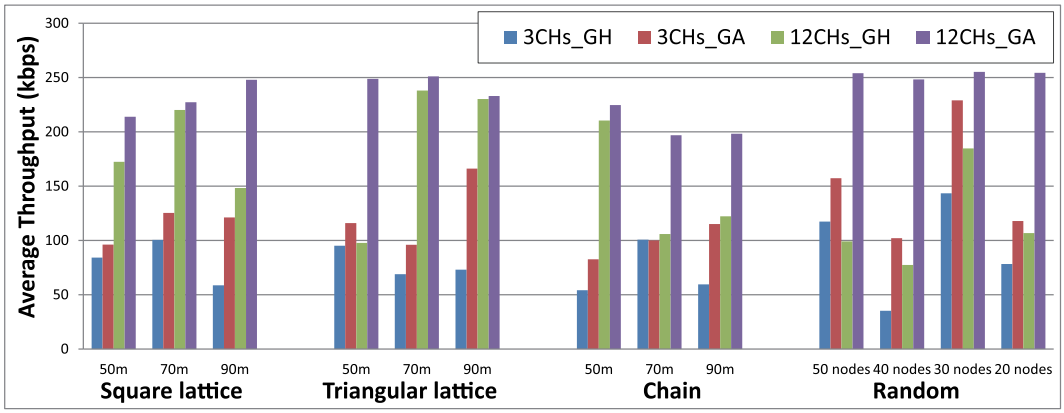

FIGURE 14. Network performance in various topologies.

The number of available channels is set to 3 or 12. At lower data rates, nearly all packets are successfully transmitted in all cases, as simultaneous transmissions are rare. However, in highly congested networks, GA demonstrates exceptional performance. At a data rate of 256 kbps, GA with 12 channels still achieves a 96.88% packet success rate. As network traffic increases, GA, with a larger number of available channels, widens the performance gap.

Fig. 14 presents simulation results in various topologies, including square lattice, triangular lattice, chain, and random. For the square and triangular lattices, 100 nodes are placed in a 10 by 10 arrangement with side lengths of 50 m, 70 m, and 90 m. In a chain topology, 25 nodes are placed at three different lengths: 50 m, 70 m, and 90 m. In a random topology, 20, 30, 40, and 50 nodes are randomly deployed in a 300 m by 300 m square region. We compare the performance of GA with GH when 3 or 12 channels are available. GA consistently outperforms GH in all cases. While GH with 12 channels may achieve a performance similar to GA in some instances, GH's performance is highly dependent on topology settings. In summary, the proposed algorithm GA, on average, demonstrates a network throughput increase of 162% and 174% compared to the greedy heuristic algorithm GH with 3 channels and 12 channels, respectively.

VI. CONCLUSION

This paper proposes channel assignment schemes aimed at mitigating network performance degradation caused by the hidden terminal, exposed terminal, and co-channel interference problems in multi-radio multi-channel wireless networks. Given the distinct transmission, interference, and carrier sensing ranges in IEEE 802.11 protocols, these issues are not only relevant to adjacent links but also extend to multi-hop links. To construct weighted conflict graphs that represent potential conflicts, we explore the relationship between hop-based distance and Euclidean distance. Leveraging the hop distance, we analyze the conditions under which each problem may arise. To the best of our knowledge, this is the first comprehensive approach to address all three problems simultaneously. We introduce the novel *Weighted Soft List Coloring* problem to tackle the channel assignment problem on the weighted conflict model and present an approximation algorithm with a worst-case ratio of 2. We prove the NP-hardness of the *Weighted Soft List Coloring* problem by defining its dual problem, Max *list*-Cut, a generalized version of the Max k-Cut problem. In simulations, we explore parameters for weights on edges of the conflict graph. Through various parameter scenarios, we observe that adjacent links are less crucial than multi-hop links as they primarily affect co-channel interference problems. Despite the network performance's reliance on topologies, we demonstrate that the proposed channel assignment achieves high performance across various topologies in simulations.

ACKNOWLEDGMENT

An earlier version of this paper was presented at the 18th International Conference on Advanced Communications Technology [1].

REFERENCES

[1] C. Lee, D. Shin, and S. Choi, "Weighted conflict-aware channel assignment in 802.11-based mesh networks," in *Proc. ICACT*, Jan. 2016, pp. 377–381.

[2] I. F. Akyildiz, X. Wang, and W. Wang, "Wireless mesh networks: A survey," *Comput. Netw.*, vol. 47, no. 4, pp. 445–487, Mar. 2005.

[3] D. Benyamina, A. Hafid, and M. Gendreau, "Wireless mesh networks design—A survey," *IEEE Commun. Surveys Tuts.*, vol. 14, no. 2, pp. 299–310, 2nd Quart., 2012.

[4] F. Hao, J. Ma, and C. Zhu, "Hidden node and interference aware channel assignment for multi-radio multi-channel wireless mesh networks," in *Proc. UIC*. Cham, Switzerland: Springer, 2011, pp. 393–404.

[5] R. Battiti, A. Bertossi, and D. Cavallaro, "A randomized saturation degree heuristic for channel assignment in cellular radio networks," *IEEE Trans. Veh. Technol.*, vol. 50, no. 2, pp. 364–374, Mar. 2001.

[6] B. Panda, M. Kumar, and S. Das, "Optimal schemes for channel assignment problem in wireless networks modeled as 2-dimensional square grids," in *Proc. IWDC*. Cham, Switzerland: Springer, 2005, pp. 298–341.

[7] H. A. Mogaibel, M. Othman, S. Subramaniam, and N. A. W. A. Hamid, "Review of channel assignment approaches in multi-radio multi-channel wireless mesh network," *J. Netw. Comput. Appl.*, vol. 72, pp. 113–139, Sep. 2016.

[8] A. B. M. A. A. Islam, M. J. Islam, N. Nurain, and V. Raghunathan, "Channel assignment techniques for multi-radio wireless mesh networks: A survey," *IEEE Commun. Surveys Tuts.*, vol. 18, no. 2, pp. 988–1017, 2nd Quart., 2016.

[9] J. So and N. H. Vaidya, "Multi-channel mac for ad hoc networks: Handling multi-channel hidden terminals using a single transceiver," in *Proc. MobiHoc*, May 2004, pp. 222–233, doi: 10.1145/989459.989487.

[10] F. Claude, R. Dorrigiv, S. Kamali, A. López-Ortiz, P. Prałat, J. Romero, A. Salinger, and D. Seco, "Broadcasting in conflict-aware multi-channel networks," in *Proc. 7th Int. Workshop Algorithms Comput. (WALCOM)*, Kharagpur, India. Cham, Switzerland: Springer, Feb. 2013, pp. 158–169.

[11] H. Skalli, S. Ghosh, S. Das, and L. Lenzini, "Channel assignment strategies for multiradio wireless mesh networks: Issues and solutions," *IEEE Commun. Mag.*, vol. 45, no. 11, pp. 86–95, Nov. 2007.

[12] B. Raman, "Channel allocation in 802.11-based mesh networks," in *Proc. IEEE INFOCOM*, vol. 6, May 2006, pp. 1–10.

[13] K. N. Ramachandran, E. M. Belding, K. C. Almeroth, and M. M. Buddhikot, "Interference-aware channel assignment in multi-radio wireless mesh networks," in *Proc. IEEE INFOCOM*, Dec. 2006, pp. 1–12.

[14] A. P. Subramanian, H. Gupta, S. R. Das, and J. Cao, "Minimum interference channel assignment in multiradio wireless mesh networks," *IEEE Trans. Mobile Comput.*, vol. 7, no. 12, pp. 1459–1473, Dec. 2008.

[15] C. Kari, Y. Kim, S. Lee, A. Russell, and M. Shin, "Soft edge coloring," in *Proc. APPROX*, 2007, pp. 189–203.

[16] W. Wang and X. Liu, "List-coloring based channel allocation for open-spectrum wireless networks," in *Proc. IEEE Veh. Technol. Conf.*, Jun. 2005, vol. 62, no. 1, p. 690.

[17] K. Jain, J. Padhye, V. N. Padmanabhan, and L. Qiu, "Impact of interference on multi-hop wireless network performance," in *Proc. 9th Annu. Int. Conf. Mobile Comput. Netw.*, Sep. 2003, pp. 66–80, doi: 10.1145/938985.938993.

[18] M. K. Marina and S. R. Das, "A topology control approach for utilizing multiple channels in multi-radio wireless mesh networks," in *Proc. 2nd Int. Conf. Broadband Netw.*, vol. 1, Oct. 2005, pp. 381–390.

[19] I. Katzela and M. Naghshineh, "Channel assignment schemes for cellular mobile telecommunication systems: A comprehensive survey," *IEEE Commun. Surveys Tuts.*, vol. 3, no. 2, pp. 10–31, 2nd Quart., 2000.

[20] D. Hammash, M. Kim, B. Lee, S. Kang, Y. Lee, and D. Lee, "HIAM: Hidden node and interference aware routing metric for multi-channel multi-radio mesh networks," in *Proc. 7th Int. Conf. Ubiquitous Inf. Manage. Commun.*, Jan. 2013, p. 107, doi: 10.1145/2448556.2448663.

[21] H.-J. Kim, M. S. Kim, and S.-J. Han, "Collision-free optimal packet scheduling algorithm for multi-hop wireless IoT networks," *Comput. Netw.*, vol. 206, Apr. 2022, Art. no. 108816.

[22] T. Yoshihiro and T. Noi, "Collision-free channel assignment is possible in IEEE802.11-based wireless mesh networks," in *Proc. IEEE Wireless Commun. Netw. Conf. (WCNC)*, Mar. 2017, pp. 1–6.

[23] T. Yoshihiro and T. Nishimae, "Practical fast scheduling and routing over slotted CSMA for wireless mesh networks," in *Proc. IEEE/ACM 24th Int. Symp. Quality Service (IWQoS)*, Jun. 2016, pp. 1–10.

[24] Y. Tian and T. Yoshihiro, "Traffic-demand-aware collision-free channel assignment for multi-channel multi-radio wireless mesh networks," *IEEE Access*, vol. 8, pp. 120712–120723, 2020.

[25] N. C. Luong, D. T. Hoang, S. Gong, D. Niyato, P. Wang, Y.-C. Liang, and D. I. Kim, "Applications of deep reinforcement learning in communications and networking: A survey," *IEEE Commun. Surveys Tuts.*, vol. 21, no. 4, pp. 3133–3174, 4th Quart., 2019.

[26] S. Wang, H. Liu, P. H. Gomes, and B. Krishnamachari, "Deep reinforcement learning for dynamic multichannel access in wireless networks," *IEEE Trans. Cognit. Commun. Netw.*, vol. 4, no. 2, pp. 257–265, Jun. 2018.

[27] K. Nakashima, S. Kamiya, K. Ohtsu, K. Yamamoto, T. Nishio, and M. Morikura, "Deep reinforcement learning-based channel allocation for wireless LANs with graph convolutional networks," *IEEE Access*, vol. 8, pp. 31823–31834, 2020.

[28] J. L. Sobrinho and A. S. Krishnakumar, "Quality-of-service in ad hoc carrier sense multiple access wireless networks," *IEEE J. Sel. Areas Commun.*, vol. 17, no. 8, pp. 1353–1368, Apr. 1999.

[29] S. Xu and T. Saadawi, "Revealing the problems with 802.11 medium access control protocol in multi-hop wireless ad hoc networks," *Comput. Netw.*, vol. 38, no. 4, pp. 531–548, Mar. 2002.

[30] J. Deng, B. Liang, and P. K. Varshney, "Tuning the carrier sensing range of IEEE 802.11 MAC," in *Proc. IEEE Global Telecommun. Conf. (GLOBECOM)*, Nov. 2004, pp. 2987–2991.

[31] K. Xu, M. Gerla, and S. Bae, "How effective is the IEEE 802.11 RTS/CTS handshake in ad hoc networks," in *Proc. Global Telecommun. Conf. (GLOBECOM)*, vol. 1, 2002, pp. 72–76.

[32] Y. Shang, W. Ruml, Y. Zhang, and M. P. J. Fromherz, "Localization from mere connectivity," in *Proc. 4th ACM Int. Symp. Mobile Ad Hoc Netw. Comput.*, Jun. 2003, pp. 201–212, doi: 10.1145/778415.778439.

[33] S. Lederer, Y. Wang, and J. Gao, "Connectivity-based localization of large scale sensor networks with complex shape," in *Proc. 27th Conf. Comput. Commun. (INFOCOM)*, Apr. 2008, pp. 789–797.

[34] V. Kann, S. Khanna, J. Lagergren, and A. Panconesi, "On the hardness of approximating MAX k-CUT and its dual," in *Proc. ISTCS*, 1996, pp. 61–67.

[35] *Network Simulator NS3*. [Online]. Available: http://www.nsnam.org

DONGHOON SHIN (Member, IEEE) received the B.S. degree in computer science and electrical engineering from Handong Global University, in 2007, and the M.S. and Ph.D. degrees in computer science from KAIST, in 2009 and 2016, respectively. He joined the National Security Research Institute as a Senior Researcher, in 2016. He has been a Professor with the Electrical Engineering and Computer Science Department, DGIST, since 2019. His research interests include computational theory, wireless networks, and information security.

CHANGREOL LEE received the B.S. degree in information and computer engineering from Ajou University, Suwon, South Korea, in 2004, and the M.S. degree in computer science from the Korea Advanced Institute of Science and Technology (KAIST), Daejeon, South Korea, in 2009. He has been a Researcher with the Inzent Research and Development Center, since 2020. His research interests include geometric problems in wireless sensor networks, computational geometry, and theory of computation.

SUNGHEE CHOI received the B.S. degree in computer engineering from Seoul National University, in 1995, and the M.S. and Ph.D. degrees in computer science from The University of Texas at Austin, in 1997 and 2003, respectively. She has been a Professor with the Computer Science Department, Korea Advanced Institute of Science and Technology (KAIST), Daejeon, South Korea, since 2004. Her research interests include computational geometry, computer graphics, and geometric problems in wireless sensor networks.